

A comparison of the multicomponent model and the mixture averaged approximation

Thesis for master of Science by Martin Torstensson

Lund Combustion Engenering - LOGE AB
and
Physics Department - Lund University

Examiner:

Carl-Erik Magnusson, Physics Department, Lund University
Claudio Verdozzi, Physics Department, Lund University

Supervisors:

Anders Borg, LOGE AB
Johan Zetterberg, Physics Department, Lund University



LUND
UNIVERSITY



Contents

1	Introduction	5
1.1	Software and data used	5
2	Theory	6
2.1	Flame terminology	6
2.2	Flame theory	6
2.3	Flame velocity	7
2.4	The Boltzmann equation	9
2.5	The collision terms	10
2.6	The Chapman-Enskog Theory . . .	10
2.7	The Stockmayer potential and the collision integrals	11
2.8	The Multicomponent Model	13
2.9	The Mixture-averaged Approxima- tion	15
2.10	Complexity of the two models . . .	16
3	Results	17
4	Discussion	18
4.1	The multicomponent model	18
4.2	The mixture averaged approximation	18
4.3	Comparison of the Mixture Aver- aged and the Multicomponent models	22
4.4	Comparison to experiment	23
4.5	Comparison to other work	23
5	Conclusion	24

Abstract

In this work the major models for calculating diffusion in simulations of a laminar premixed hydrogen flame, the mixture averaged approximation and the multicomponent model, are explained and compared. This is done in order to see if the accuracy gained in implementing the multicomponent model is enough to warrant the increased workload the transition will cause.

The models are used to calculate the mean flame speed for a hydrogen flame, as that is the one most easily measured in experiments. But the results are inconclusive in comparison with experiment, since thermal diffusion was not implemented. Still, it does show a clear distinction between the results produced by the two models, as the mixture averaged model gives the flame speed as 239 cm/s while the multicomponent gives it as 250 cm/s, for a stoichiometric hydrogen flame with standard temperature and pressure.

The calculation time is also significantly different, as the multicomponent calculation took 42 minutes, while the mixture averaged calculations only took 17 minutes. Worth noting is that the mixture averaged model was heavily optimized, which explains some of the difference.

Acknowledgements

I would first start to thank my two supervisors Anders Borg and Johan Zetterberg for their help along the way, and for their patience with me. Also Harry Lethiniemi and Karin Fröjd for their help in reasoning and answering questions. Lastly my family and my friend Rebecca Forsmark, without whom this work probably never would have been finished.

1 Introduction

Combustion may be one of humankind's oldest technologies, but it is still responsible for around 80-90% of the energy consumption in the modern society e.g., heating, electric power, transport. This means that it is important to understand the process, to be able to make it as efficient and safe as possible. Even as we strive to get away from fossil fuels, many combustion processes are just shifted to renewable fuels, so combustion will be with us for a long time.

The central part of combustion is the flame. Since the flame process is a complicated process, which includes radicals that are highly reactive and thereby short lived, it is hard to measure everything in practice. Because of this, simulations are used as a complement to experiments. To get an indication of whether the simulated result is close to what actually goes on in the flame, one or more measurable properties, e.g. the *flame speed*, are compared to their experimental values. The flame speed is the speed with which the flame will propagate in a homogeneous combustible mixture. It is often measured and documented, and depends on some of the important parts of the calculation, so it is a good indicator that the simulation is close to reality. It is also dependent on the diffusion, and is therefore a good measure of the results of the simulations made in this work.

A typical flame to simulate is a *laminar premixed flame*. That it is *laminar* means that it has only one, clearly defined, direction of propagation, the opposite being a *turbulent flame*. An example of a laminar flame is the center of a Bunsen burner, away from any edge effects, it burns in only one direction, straight up. *Premixed* means that fuel and oxygen is mixed before reaching the flame, also as in a Bunsen burner. It is not mixed in the flame, as in a candle. Since it is relatively easy to control the fuel-oxygen-ratio of a premixed gas, and change the gas velocity to match the flame speed, it is one of the easiest flames to measure the flame speed of. It is also a useful flame, as it can be used as an approximation for very many things, from gasoline engines to Bunsen burners. In this work all flames simulated were premixed laminar hydrogen flames.

Two different ways to calculate diffusion, the multicomponent model and the mixture averaged approximation, are compared in this work. This is in part to see if the multicomponent model can be easily implemented as an alternative to the mixture averaged approximation, and if it is accurate enough to be worth the extra calculation time.

1.1 Software and data used

The simulation software used in this work is called Chamble, part of the commercial software DARS owned by DigAnaRS [1]. Chamble uses the mixture averaged approximation as standard, but was modified to use the multicomponent model as well. It gets the chemical and physical properties of the species from files, based mainly on experiments.

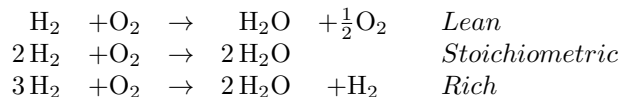
2 Theory

This section starts with some basic flame theory, and then the theory needed to understand the two different diffusion models are presented. At the end of the section, the two models themselves are presented.

2.1 Flame terminology

In combustion sciences, there are some terms used to describe different flames. First, the fuel can be *premixed* with the oxygen, or *non-premixed*. Secondly the flame can be *turbulent* or *laminar*. These concepts were introduced in chapter 1.

Flames can also be fuel-rich or fuel-lean, depending on if there is an excess of fuel or oxygen. If the fuel and oxygen ratios are such that all the fuel and all the oxygen get depleted in the process, the flame is said to be *stoichiometric*.



To describe the ratio between the fuel and the air in a way that is suitable for the combustion process, the ratio is weighted against the stoichiometric ratio, thus making sure that it is easy to see if the mix is lean, rich or stoichiometric. This weighted ratio is called *fuel equivalence ratio* and is defined as

$$\Phi = \frac{\frac{X_{fuel}}{X_{O_2}}}{\frac{X_{fuel, stoich}}{X_{O_2, stoich}}} \quad (2.1)$$

where X_i is the mole fraction of the species i , defined as

$$X_i = \frac{n_i}{n_{tot}} \quad (2.2)$$

where n_i is the number of molecules of species i in a volume, and n_{tot} is the total number of molecule in the same volume. With this definition $\Phi = 1$ means that the flame is stoichiometric, $\Phi > 1$ means that the flame is rich and $\Phi < 1$ means that it is lean.

The *flame speed* is the speed of the unburned mixture in system where the flame is stationary.

2.2 Flame theory

When simulating flames, two things are of prime importance. The first is to know where everything is, and the second were it is going. Since the goal of this work is to study what effect different methods of calculating the diffusion has on the flame velocity, it is important that that relation is clear.

In all the simulations of this work, the flames are expected to be stationary. To that end, there are three quantities that must be accounted for. First the

total mass is to be conserved, so the mass transport has to be constant in space [2]

$$\frac{\partial(\rho v)}{\partial z} = 0 \quad (2.3)$$

where ρ is the density, v the velocity of the gas and z the velocity direction. To get the density, the gas is considered near enough ideal and the ideal gas law is used.

Secondly, the mass of each species needs to be accounted for. This is done by looking at the species' mass as it is transported or transformed [2]

$$\frac{\partial j_i}{\partial z} - \rho v \frac{\partial Y_i}{\partial z} + r_i = 0 \quad (2.4)$$

where j_i is the diffusion flux of species i relative to the average mass velocity, $Y_i = \frac{m_i}{m}$ is the mass fraction of species i , m_i is the mass of species i and m is the mass of the mixture, and r_i represents the chemical reactions. The first term is the mass change of species i due to diffusion, the second term is the mass change of species i due to the macroscopical flow, and the last term corresponds to the mass change of species i due to chemical reactions.

Finally, the total energy needs to be conserved. This is done by looking at the temperature difference and how that relates to energy being transported and released in chemical processes [2]

$$\frac{\partial}{\partial z} \left(\lambda \frac{\partial T}{\partial z} \right) - \left(\rho v c_p + \sum_i j_i c_{p,i} \right) \frac{\partial T}{\partial z} - \sum_i h_i r_i = 0 \quad (2.5)$$

where λ is the thermal conductivity of the mixture, T is the temperature of the mixture, c_p is the specific heat constant for the mixture, $c_{p,i}$ is the specific heat constant for species i , and h_i is the specific enthalpy of species i . In analogy with above, the first term is the thermal energy that travels due to thermal conduction, the second term is the thermal energy that traveling species carry with them and the last part is the change in thermal energy due to chemical reactions. These sets of equations are then solved for T , Y_1 , Y_2, \dots and v using the boundary conditions based on that the initial Y_i and T are known, and since the model uses radiation, that their curvature is constant, i.e.

$$\begin{aligned} \frac{\partial^2 Y_i}{\partial z^2} &= 0 \\ \frac{\partial^2 T}{\partial z^2} &= 0 \end{aligned} \quad (2.6)$$

Finally, the assumption that at a given point in the flame, the temperature will have increased by 30 % from the initial T . Initial is, in this context, taken to mean "spatially before the flame", since the equations are time independent.

2.3 Flame velocity

Calculating the flame velocity usually means solving a system of differential equations, most often by numerical methods. But in order to use an approximate

model to give some indication to how it will behave, a presentation of Zeldovich's flame analysis will follow. This model were created by Zeldovich and Frank-Kamenetskii in 1938 [2].

Starting of with two of the conservation equations (2.4) and (2.5) the assumption that all the chemical kinetics can be simulated by a one-step global reaction with the first order reaction rate needs to be made

$$r = -\rho Y_{\mathcal{F}} A e^{-\frac{E_{act}}{RT}} \quad (2.7)$$

where $Y_{\mathcal{F}}$ is the mass fraction for the fuel, A is the preexponential factor, which is an empirically verified factor. E_{act} is the activation energy and R is the gas constant. The three quantities λ , c_p and ρD , where ρD is the diffusion coefficient since D is the mass diffusivity, are expected to be constant in space and the sum of different diffusion velocities times different specific heat transfers $\sum_j V_j c_{p,j}$ is assumed negligible. With these approximations applied to (2.4) and (2.5), and denoting the fuel with \mathcal{F} and the product with \mathcal{P} , they turn into

$$D \frac{\partial^2 Y_{\mathcal{F}}}{\partial z^2} - v \frac{\partial Y_{\mathcal{F}}}{\partial z} - Y_{\mathcal{F}} \cdot A \cdot e^{-\frac{E_{act}}{RT}} = 0 \quad (2.8)$$

$$\frac{\lambda}{\rho c_p} \frac{\partial^2 T}{\partial z^2} - v \frac{\partial T}{\partial z} + Y_{\mathcal{F}} \frac{h_{\mathcal{P}} - h_{\mathcal{F}}}{c_p} \cdot A \cdot e^{-\frac{E_{act}}{RT}} = 0 \quad (2.9)$$

Through examining experimental data, the assumption that the mass diffusivity D and the thermal diffusivity $\frac{\lambda}{\rho c_p}$ are roughly the same seems reasonable [2]. This means that now (2.8) and (2.9) are almost the same. Substituting the enthalpy with the temperature in 2.8, via

$$\delta = T_b - T = \left[\frac{h_{\mathcal{P}} - h_{\mathcal{F}}}{c_p} \right] Y_{\mathcal{F}} \quad (2.10)$$

where T_b is the temperature of the burnt gas, gives

$$D \frac{d^2 \delta}{dz^2} - v \frac{d\delta}{dz} - \delta \cdot A \cdot e^{-\frac{E_{act}}{R(T_b - \delta)}} = 0 \quad (2.11)$$

Now 2.11 is the same as 2.9.

The solution of (2.11) is complicated, but it can be shown that a solution exists only if v has an eigenvalue, called *flame velocity*, that is

$$v_L = \sqrt{\frac{D}{\tau}} \quad (2.12)$$

where $\tau = [A \cdot \exp(-E/RT)]^{-1}$ is a characteristic reaction time at temperature $T < T_b$. In this model the flame velocity depends only on the characteristic reaction time and the diffusivity (this is a simplified model that does not take radiation into account, so mass and energy diffusion are equivalent). This is of course a very simplified model, but it shows the importance of being able to calculate the diffusion terms accurately.

2.4 The Boltzmann equation

To describe the particles in a gas, the velocity distribution function $f(\mathbf{r}, \mathbf{p}, t)$, where \mathbf{r} is position, \mathbf{p} is momentum and t is time, is used. It describes the amount of particles in the small phase space region of $f(\mathbf{r}, \mathbf{p}, t) d\mathbf{r}d\mathbf{p}$. This means that for a gas with N particles, it is dependent on $6N + 1$ variables, i.e. the three dimensional positions \mathbf{r} and momenta \mathbf{p} of all the particles in the gas and the time. This makes it almost impossible to express the function in full, but it is still applicable to derive an approximation, and that is what the Boltzmann equation is.

Looking at a gas with the species \mathcal{S} , and specifically the specie $i \in \mathcal{S}$, if the gas is subject to an external force \mathbf{F}_i but no internal interactions, then the particles of species i that occupy the space $f_i(\mathbf{r}, \mathbf{p}, t) d\mathbf{r}d\mathbf{p}$ a short time later will occupy the space $f_i\left(\mathbf{r} + \frac{1}{m_i}\mathbf{p}dt, \mathbf{p} + \mathbf{F}_i dt, t + dt\right) d\mathbf{r}d\mathbf{p}$, where m_i is the mass of a particle of species i . This means that, without collisions

$$f_i\left(\mathbf{r} + \frac{\mathbf{p}}{m_i}dt, \mathbf{p} + \mathbf{F}_i dt, t + dt\right) d\mathbf{r}d\mathbf{p} = f_i(\mathbf{r}, \mathbf{p}, t) d\mathbf{r}d\mathbf{p} \quad (2.13)$$

This is of course not true if the particles interact with each other. If the time spent interacting with other molecules is considered only a small part of the particles' lifetime, the assumption that only binary collisions are relevant can be made. Then collisions will cause some of the particles that started up inside the first region to end up outside of the second, and some particles starting outside the first region will, due to collisions, end up inside the second. To account for this, the collision terms $\Gamma_{ij}^{(+)}$ and $\Gamma_{ij}^{(-)}$ are added, to account for adding and subtracting particles of species i due to collisions with particles of species j , respectively. This turns 2.13 into

$$f_i\left(\mathbf{r} + \frac{\mathbf{p}}{m_i}dt, \mathbf{p} + \mathbf{F}_i dt, t + dt\right) d\mathbf{r}d\mathbf{p} = f_i(\mathbf{r}, \mathbf{p}, t) d\mathbf{r}d\mathbf{p} + \sum_{j \in \mathcal{S}} \left[\Gamma_{ij}^{(+)} - \Gamma_{ij}^{(-)} \right] d\mathbf{r}d\mathbf{p}dt \quad (2.14)$$

If the left hand side is Taylor expanded with respect to dt and only the first order terms are kept, this gives

$$\begin{aligned} f_i\left(\mathbf{r} + \frac{\mathbf{p}}{m_i}dt, \mathbf{p} + \mathbf{F}_i dt, t + dt\right) &= \\ &= \left[f_i(\mathbf{r}, \mathbf{p}, t) + \frac{\mathbf{p}}{m_i}dt \frac{\partial f_i}{\partial \mathbf{r}} + \mathbf{F}_i dt \frac{\partial f_i}{\partial \mathbf{p}} + dt \frac{\partial f_i}{\partial t} \right] d\mathbf{r}d\mathbf{p} \end{aligned} \quad (2.15)$$

Now combining 2.14 with 2.15, subtracting $f_i(\mathbf{r}, \mathbf{p}, t) d\mathbf{r}d\mathbf{p}$ from both sides and dividing by $d\mathbf{r}d\mathbf{p}$, this turns into the Boltzmann equation

$$\frac{\partial f_i}{\partial t} + \frac{1}{m_i} \left(\mathbf{p} \cdot \frac{\partial f_i}{\partial \mathbf{r}} \right) + \left(\mathbf{F}_i \cdot \frac{\partial f_i}{\partial \mathbf{p}} \right) = \sum_j \left[\Gamma_{ij}^{(+)} - \Gamma_{ij}^{(-)} \right] \quad (2.16)$$

2.5 The collision terms

Since the collision terms $\Gamma_{ij}^{(-)}$ specify all collisions that cause the particles at $(\mathbf{r}, \mathbf{p}, t)$ to not end up in $(\mathbf{r} + \frac{\mathbf{p}}{m_i} dt, \mathbf{p} + \mathbf{F}_i dt, t + dt)$, they relate to all particles that are close enough to collide with the i -molecules from $(\mathbf{r}, \mathbf{p}, t)$ during the time dt . This is described by

$$\Gamma_{ij}^{(-)} = \iint f_i f_j |\mathbf{g}_{ij}| \alpha_{ij} d\hat{\mathbf{e}}' d\mathbf{p}_j \quad (2.17)$$

were $\mathbf{g}_{ij} = \frac{\mathbf{p}_j}{m_j} - \frac{\mathbf{p}_i}{m_i}$ is the relative velocity vector, $\hat{\mathbf{e}}'$ is a unit vector in the direction of \mathbf{g}'_{ij} , where the apostrophe marks that it is after the collision, and α_{ij} is a positive scalar that is defined as

$$\alpha_{ij} = \frac{b \left| \frac{\partial b}{\partial \chi} \right|}{\sin \chi} \quad (2.18)$$

b is the offset of the collision and χ is the polar angle between the relative velocities before and after the collision. Here both the subscript i and j are used, as the particles that are close by can be of a different species than that of the particle originally looked at. This will affect the potential experienced by the colliding particles, and will be discussed more in 2.7.

The second group of collision terms corresponds to collisions that push molecules not in the original volume into the volume $(\mathbf{r} + \frac{\mathbf{p}_i}{m_i} dt, \mathbf{p}_i + \mathbf{F}_i dt)$ by time $t + dt$. Those terms is described by

$$\Gamma_{ij}^{(+)} = \iint f'_i f'_j |\mathbf{g}_{ij}| \alpha_{ij} d\hat{\mathbf{e}} d\mathbf{p}_j \quad (2.19)$$

were f' is the velocity distribution function after the collision. Using this in equation (2.16), the Boltzmann equation becomes

$$\frac{\partial f_i}{\partial t} + \frac{1}{m_i} \left(\mathbf{p}_i \cdot \frac{\partial f_i}{\partial \mathbf{r}} \right) + \left(\mathbf{F}_i \cdot \frac{\partial f_i}{\partial \mathbf{p}_i} \right) = \sum_j \iint (f'_i f'_j - f_i f_j) |\mathbf{g}_{ij}| \alpha_{ij} d\hat{\mathbf{e}} d\mathbf{p}_j \quad (2.20)$$

were the left side is due to normal movement and the right side is due to collisions. This can also be written as $\mathfrak{D}_i(f_i) = \sum_j \mathfrak{B}_{ij}(f_i, f_j)$, were $\mathfrak{D}_i(f_i)$ is the normal movement part and $\sum_j \mathfrak{B}_{ij}(f_i, f_j)$ is the collision part. It is usually written in terms of velocity rather than momentum, and then turns into

$$\frac{\partial f_i}{\partial t} + \left(\mathbf{v}_i \cdot \frac{\partial f_i}{\partial \mathbf{r}} \right) + \frac{1}{m_i} \left(\mathbf{F}_i \cdot \frac{\partial f_i}{\partial \mathbf{v}_i} \right) = \sum_j \iint (f'_i f'_j - f_i f_j) |\mathbf{g}_{ij}| \alpha_{ij} d\hat{\mathbf{e}} d\mathbf{v}_j \quad (2.21)$$

2.6 The Chapman-Enskog Theory

At the start of last century, Sidney Chapman and David Enskog independently worked on a solution to the Boltzmann equation. Their theories were later

merged into the Chapman-Enskog Theory. They assumed that the Boltzmann equation could be expressed as a sum of functions $f_i = f_i^0 + f_i^1 + \dots$, each term bringing the total closer to the actual value [3]. Expressing the Boltzmann equation as

$$\xi_i(f_i) = 0 \quad (2.22)$$

were $\xi_i(f_i) = \mathfrak{D}_i(f_i) - \sum_j \mathfrak{B}_{ij}(f_i, f_j)$, they assumed that there would be a way to divide ξ so that the n :th term only depends on the first n terms in the f_i -sum

$$\xi_i(f_i) = \xi_i(f_i^0 + f_i^1 + \dots) = \xi_i^0(f_i^0) + \xi_i^1(f_i^0, f_i^1) + \xi_i^2(f_i^0, f_i^1, f_i^2) + \dots \quad (2.23)$$

Now, since $\xi_i(f_i) = 0$, and the subdivision in 2.23 is not unique, the constraint that all the terms ξ_i^k should be zero is not an impossible one. This changes 2.22 from one equation with an infinite number of unknowns to an infinite number of equations, but each only introducing one new unknown. Also, since each equation takes the result closer to the real value, only a limited number of them needs to be solved to get an approximation of the result.

The subdivision made it possible to express the first term of the function as a Maxwellian distribution

$$f_i^0 = \rho_i \left(\frac{m_i}{2\pi k_B T} \right)^{\frac{3}{2}} \exp \left(-\frac{m_i (v_i - v_0)^2}{2k_B T} \right) \quad (2.24)$$

were ρ_i is the density of the species i , k_B is Boltzmann's constant and v_0 is the local mass averaged velocity.

The second term to f is expressed as

$$f_i^1 = f_i^0 \Phi_i \quad (2.25)$$

were Φ_i is a scalar function with three parts. The first part is dependent on the gradient of the logarithm of the temperature, the second is dependent on the gradient of the mean mass velocity of the total gas, and the third is dependent on the gradient of the pressure of each gas component [3]. When looking at the diffusion, the first part relates to the thermal diffusion and the last part to regular diffusion.

2.7 The Stockmayer potential and the collision integrals

When calculating the collision terms, as seen in 2.5, the scattering of different collisions first needs to be calculated. To do this, the interaction potential needs to be known. Since many species that are common in combustion are dipoles, it is a good idea to have a potential taking that into account. The standard potential for this is the Stockmayer potential [4, 5]

$$\phi(r) = 4\epsilon_{ij} \left(\left(\frac{\sigma_{i,j}}{r} \right)^{12} - \left(\frac{\sigma_{i,j}}{r} \right)^6 \right) - \left(\frac{\mu_1 \mu_2}{r^3} \right) \zeta \quad (2.26)$$

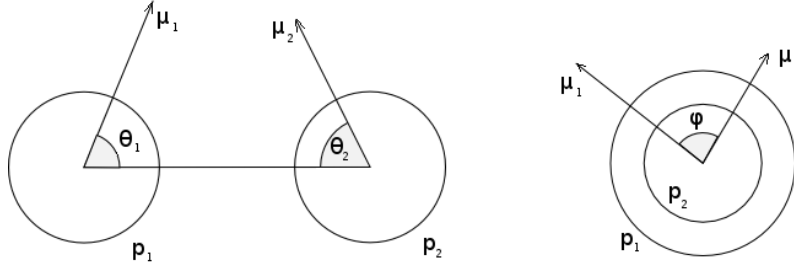


Figure 2.1: The variables in the Stockmayer potential. The left part is seen from the side, while the right part are the same particles seen from the right.

where ϵ_{ij} is the characteristic collision energy between species i and j , $\sigma_{i,j}$ is the cross-section for the collision, r is the distance between the molecules, μ_i is the dipole moment of molecule i , and ζ is defined as

$$\zeta = 2 \cos \theta_1 \cos \theta_2 - \sin \theta_1 \sin \theta_2 \cos \phi \quad (2.27)$$

where θ_1 and θ_2 are the angles between the respective dipole moments and the line that connects the center of the two molecules, and ϕ is the azimuthal angle between them, see figure 2.1. It can be noted that if one of the particles is without dipole moment, the Stockmayer potential turns into the well known Lennard-Jones 12-6 potential[5].

Using the potential, the angle of deflection can be calculated from the classical expression

$$\chi(b, g) = \pi - 2b \int_{r_m}^{\infty} \left(1 - \frac{\phi}{m_{ij} g_{ij}^2 / 2} - \frac{b^2}{r^2} \right)^{-1/2} \frac{dr}{r^2} \quad (2.28)$$

where $m_{ij} = m_i m_j / (m_i + m_j)$ is the reduced mass and r_m is the minimum approach distance, defined through

$$\phi(r_m) = \frac{m_{ij} g_{ij}^2}{2} \left(1 - \frac{b^2}{r_m^2} \right) \quad (2.29)$$

In order to calculate the deflection angle with a potential that differentiates between different angles, without knowing all the particles orientations, some assumptions need to be made. In an early attempt to solve the problem, Krieger tried to put ζ to a fixed value of 2, but it was later shown that his good results only related to an error in his calculations and this model has been discarded[4].

Instead Monchick and Mason [4] tried to use a mean value, which gave good results. They based their work on two assumptions; the first is that the

rotational energy is small compared to the kinetic energy, which means that the inelastic collisions, where kinetic energy is transferred to rotational, can be neglected. Their justification for this is that most energy transferred to rotational is only one rotational quantum, which in turn is much less than the mean kinetic energy of the molecules in the gas, which is $\frac{3}{2}k_B T$. This does not work well when dealing with quantities that are concerned specifically with internal energy, such as the thermal conductivity, but will suffice when dealing with diffusion.

The second assumption concerns the orientation-dependent potential. Although the potential is acting on the molecules during the whole trajectory, Monchick and Mason suggested that the angle is most relevant only for a short period, when the molecules are closest to each other. This means that instead of looking at all possible trajectories, they were only concerned with looking at the relative angle during impact, and that angle was considered to be static.

Using this assumption, an average of the possible outcomes could be calculated, and that is done by the collision integral

$$\Omega_{i,j}^{(k,l)} = \sqrt{\frac{2\pi k_B T}{m_{i,j}}} \int_0^\infty \int_0^\infty e^{-\hat{g}^2} \hat{g}^{(2l+3)} \left[1 - (\cos \chi)^k\right] b db d\hat{g} \quad (2.30)$$

where k and l are two integer parameters that relate the collision integral to different modes of transportation and $\hat{g} = g\sqrt{m_{i,j}/2k_B T}$. Now introducing the reduced temperature and reduced dipole moment

$$T_{i,j}^* = \frac{k_B T}{\epsilon_{i,j}} \quad (2.31)$$

$$\mu_{i,j}^* = \frac{1}{2} \frac{\mu_i \mu_j}{\epsilon_{i,j} \sigma^3} \quad (2.32)$$

and then normalizing the collision integral to the collision integral for the hard sphere, the result is the non-dimensional reduced collision integral, $\Omega_{i,j}^{(k,l)*}(T_{i,j}^*, \mu_{i,j}^*)$, that is a function of only two parameters, and can be tabulated, as Monchick and Mason did[4]. This is then used in the expression for the binary diffusion coefficient;

$$\mathcal{D}_{ij} = \frac{3}{16} \frac{\sqrt{2\pi (k_B T)^3 / m_{ij}}}{p \pi \sigma_{i,j}^2 \Omega_{i,j}^{(1,1)*}(T_{i,j}^*, \delta_{i,j}^*)} \quad (2.33)$$

where p is the pressure.

2.8 The Multicomponent Model

The multicomponent model as described by Ern and Giovangigli[6] is a more exact solution of the Boltzmann equation compared to the mixture-averaged approximation to be described later. Their solution is interesting since it takes energy levels into account, although that is not implemented in this work. This is a necessary exclusion, since the energy levels were not implemented in the

chemical data, but also a justifiable exclusion since the change in internal energies due to collisions are much smaller than the thermal energies. Hence, it should only have a small effect on the result, and is not a necessary inclusion in this study.

The solution presented by Ern and Giovangigli is symmetric, which facilitates the solving of the equations, and using all the methods fully would decrease the complexity significantly. Unfortunately, due to time restraints on this work that was not implemented, and thereby the complexity is still n^3 .

Ern and Giovangigli start by using the Chapman-Enskog method of solving the Boltzmann equation, then they subdivided $\Phi = \{\Phi_i\}_{i \in \mathcal{S}}$ into parts, where Φ^{D_i} is the part related to the diffusion, and then expressed that as

$$\Phi^{D_i} = \sum_{r=0,1} \sum_{j \in \mathcal{S}} \alpha_j^{rD_i} \xi^{rj} \quad (2.34)$$

where \mathcal{S} is a set containing all the relevant species, ξ^{rj} are a set of carefully chosen basis functions and $\alpha_j^{rD_i}$ is a set of scalar coefficients that relate Φ^{D_i} to the basis functions. $\alpha_j^{rD_i}$ relates to the diffusion coefficient through

$$\alpha_j^{0D_i} = D_{ij} \quad (2.35)$$

Then they used a variational procedure to get the equation

$$L\alpha^{D_i} = \beta^{D_i} \quad (2.36)$$

where L is a symmetric, positive definite $2n \times 2n$ matrix derived from the basis functions, α^{D_i} is a vector with the elements $\left\{ \left\{ \alpha_j^{0D_i} \right\}_{j \in \mathcal{S}} ; \left\{ \alpha_j^{1D_i} \right\}_{j \in \mathcal{S}} \right\}$ and β^{D_i} is a $2n$ 'th order vector derived from the basis functions and the functions $\Psi = \left\{ -\mathfrak{D} (\log f_i^0) \right\}_{i \in \mathcal{S}}$, and related to the mass-fractions by

$$\begin{cases} \beta_j^{0D_i} = \delta_{ij} - Y_j & i, j \in \mathcal{S} \\ \beta_j^{1D_i} = 0 & i, j \in \mathcal{S} \end{cases}$$

L is expanded to

$$L = \begin{pmatrix} L^{00} & L^{01} \\ L^{10} & L^{11} \end{pmatrix} \quad (2.37)$$

where the elements of the sub-matrices are

$$L_{ii}^{00} = \sum_{\substack{j \in \mathcal{S} \\ j \neq i}} \frac{X_i X_j}{\mathcal{D}_{ij}} \quad i \in \mathcal{S} \quad (2.38)$$

$$L_{ij}^{00} = -\frac{X_i X_j}{\mathcal{D}_{ij}} \quad i, j \in \mathcal{S}, i \neq j \quad (2.39)$$

$$L_{ii}^{01} = \sum_{\substack{j \in \mathcal{S} \\ j \neq i}} \frac{X_i X_j}{\mathcal{D}_{ij}} \frac{m_i}{m_i + m_j} (6\bar{c}_{ij} - 5) \quad i \in \mathcal{S} \quad (2.40)$$

$$L_{ij}^{01} = \frac{X_i X_j}{2\mathcal{D}_{ij}} \frac{m_i}{m_i + m_j} (6\bar{c}_{ij} - 5) \quad i, j \in \mathcal{S}, i \neq j \quad (2.41)$$

$$L_{ii}^{11} = \sum_{\substack{j \in \mathcal{S} \\ j \neq i}} \frac{X_i X_j}{\mathcal{D}_{ij}} \frac{m_i m_j}{(m_i + m_j)^2} \left[\frac{15}{2} \frac{m_i}{m_j} + \frac{25}{4} \frac{m_j}{m_i} - 3 \frac{m_j}{m_i} \bar{B}_{ij} + 4\bar{A}_{ij} \right] \quad i \in \mathcal{S}$$

$$L_{iji}^{11} = -\frac{X_i X_j}{\mathcal{D}_{ij}} \frac{m_i m_j}{(m_i + m_j)^2} \left[\frac{55}{4} - 3\bar{B}_{ij} - 4\bar{A}_{ij} \right] \quad i, j \in \mathcal{S} \quad i \neq j \quad (2.42)$$

and $L^{10} = (L^{01})^T$. \bar{A}_{ij} , \bar{B}_{ij} and \bar{C}_{ij} are defined as

$$\bar{A}_{ij} = \frac{1}{2} \frac{\Omega_{ij}^{(2,2)}}{\Omega_{ij}^{(1,1)}} \quad (2.43)$$

$$\bar{B}_{ij} = \frac{1}{3} \frac{5\Omega_{ij}^{(1,2)} - \Omega_{ij}^{(1,3)}}{\Omega_{ij}^{(1,1)}} \quad (2.44)$$

$$\bar{C}_{ij} = \frac{1}{3} \frac{\Omega_{ij}^{(1,2)}}{\Omega_{ij}^{(1,1)}} \quad (2.45)$$

There are some efficient ways to do this, but in this work the theory up to this point was the main focus, and the more effective ways were not explored.

2.9 The Mixture-averaged Approximation

In the mixture-averaged approximation, the diffusion velocity for each gas is calculated by approximating all the other gases' velocities as the same. That means that instead of calculating the diffusion term D_{ij} for each couple of gases, only one diffusion term, D'_{im} , is calculated for each species.

Starting with the assumption[7]

$$V_i = -\frac{1}{X_i} D'_{im} \nabla X_i \quad (2.46)$$

where $X = \frac{n_i}{n}$ is the mole fraction of species i , and V_i is the speed of specie i relative to the mean mass speed, i.e.

$$V_i = \tilde{V}_i - V = \tilde{V}_i - \sum_j \tilde{V}_j Y_j \quad (2.47)$$

V is the mean speed of the mass in the center of mass frame of reference, and \tilde{V}_i is the mean speed of species i in the laboratory frame of reference. Combining (2.46) and (2.47), the gradient of the mole fraction can be expressed as

$$\nabla X_i = -\frac{X_i \left(\tilde{V}_i - \sum_j \tilde{V}_j Y_j \right)}{D'_{im}} \quad (2.48)$$

Using the Stefan-Maxwell formula[7]

$$\nabla X_i = -\sum_j \frac{X_i X_j}{D_{ij}} \left(\tilde{V}_i - \tilde{V}_j \right) \quad (2.49)$$

where D_{kj} are the binary diffusion coefficients, the combination of (2.48) and (2.49) yields

$$\frac{X_i \left(\tilde{V}_i - \sum_j \tilde{V}_j Y_j \right)}{D'_{im}} = \sum_j \frac{X_i X_j}{D_{ij}} \left(\tilde{V}_i - \tilde{V}_j \right) \quad (2.50)$$

Applying the mixture averaged approximation, that $V_i = V_j, \forall i \neq j$, and rearranging yields

$$D'_{im} = \frac{1 - Y_i}{\sum_{j \neq i} X_j / D_{ji}} \quad (2.51)$$

As can be seen, (2.51) makes the diffusion coefficient only depend on things which are easily calculated, while the speed terms, which are complicated to calculate, have been removed.

2.10 Complexity of the two models

One of the things to keep in mind when working with simulations is the computation time. The computation time is dependent on both the type of model used, and a series of other factors, as the numbers of chemicals considered in a flame simulation. The number of chemicals varies depending on fuel, and can be from as few as six, if the fuel is hydrogen, up to well over a thousand if the fuel is a carbohydrate fuel, the latter being common in fossil fuels. To discuss how different models' calculation time react with an increasing number of chemicals, the concept of *scaling* is introduced. If a model scales as n , it means that if the number of chemicals is doubled, the calculation time is doubled as well. On the other hand, if the model scales as n^2 , the calculation time is quadrupled if the number of chemicals are doubled, since $2^2 = 4$.

Since the mixture averaged approximation requires the inversion of a matrix that is $2n \times 2n$, see section 2.8, that has a base scaling of n^3 [8]. The matrix has some symmetries so the scaling can be taken down to the order of n [6], but that is not fully implemented in this work.

On the other hand, the mixture averaged approximation treats one species at the time, and treats all the others as a homogeneous mixture. This means that it scales as n .

3 Results

In this work, focus has been given to the influence three variables have on the flame speed within the two models. These three variables are the fuel equivalence ratio, the starting temperature and the pressure. Since it is difficult to examine the effect of these three variables at the same time, they have been examined one at a time instead. First the calculations of the flame speed depending on the fuel equivalence ratio is presented in figure 3.1, where it is also compared to the experimental measurements of the flame speed presented in [9]. The pressure and temperature are set to standard values ($T = 298 K$, $P = 101.3 kPa$). All simulations are done without thermal diffusion.

The first thing that can be seen is that neither result is a close fit to the experimental values for low Φ . The mixture-averaged approximation comes marginally closer, but for $1 < \Phi \leq 2$ neither is close to the experiment's results. These results are also confirmed by table 3.1, that once again compares the calculations to the values presented in [9]. It is also worth noting that the multicomponent calculation returns higher values for the flame speed almost for all Φ , although for $\Phi \geq 0.5$, the difference between the two calculations is never greater than 3%.

The simulations with varying initial pressure are not compared to any experimental values, since none have been found. Here a stoichiometric mixture is used, and the initial temperature is room temperature ($T = 298 K$). As can be seen in the figure 3.2, the flame speed calculated with the multicomponent model is higher here as well, but never goes higher than 3% more than the mixture averaged, with a peak in the (relative) difference around normal air pressure.

In the plot showing the temperature variation simulation, figure 3.3, a stoichiometric mixture and normal air pressure is used. It can be seen that the multicomponent values are still higher, but the relative difference between the two methods is increasing steadily, from about 2.7% to the left of the plot (250 K) to about 3.5% to the right (600 K).

Next, the mass flux is considered directly. The mass fluxes of the radicals and that of the H_2O and O_2 basically have the same shape, independent of which model is used in the calculation. It is just shifted or scaled. But the diagrams for both the H_2 molecule, figure 3.5 a), and the N_2 molecule, figure 3.5 d), show some differences. In the hydrogen molecule there is a discrepancy in the first part of the plot, where the mixture averaged approximation calculates a higher value than the multicomponent. Despite this, they still agree quite well after 0.12 mm. But the difference differentiates the two curves from each other.

The other mass flux that differs is the nitrogen, where the mixture averaged predicts that the nitrogen diffusion mass flux should move nitrogen away from the point 0.08 mm from zero. This despite the fact that nitrogen, as opposed to every other species considered here, is not reacting in these simulations. This gives the effect that unlike the oxygen radical, which shows a similar curve, the nitrogen can not be created at the point it flees from. In the Multicomponent model, the nitrogen is mostly accelerated to the right, although a small section

Table 3.1: Flame speed

ϕ	$S_L(mm/s)$	MC(mm/s)	MA(mm/s)
0.30	180	100	119
0.45	470	613	642
0.60	910	1295	1268
0.75	1360	1891	1805
0.90	1700	2319	2206
1.05	2030	2598	2480
1.20	2280	2755	2650
1.50	2500	2810	2755
1.65	2540	2754	2729
1.80	2490	2680	2674
2.10	2360	2463	2518
2.35	2290	2283	2373
2.60	2060	2114	2227
3.00	1830	1853	1998

before the 0-point is accelerated to the left.

4 Discussion

This is started with a short discussion of the two models, followed by comparisons between them, to experiment and to other work.

4.1 The multicomponent model

This is the more precise model for calculating the gas properties. As such, it is also the more computational demanding. Since all species interact, the system scales at least as n^2 , but in this application, it scales as n^3 since it is based on inverting a $n \times n$ -matrix. This might not seem like much when dealing with combustion of hydrogen, which uses nine species, but when calculating the combustion of long carbon chains, the number of species can reach into the hundreds. On the other hand, it is a more exact model, and as such should give more precise answers.

4.2 The mixture averaged approximation

Since the main approximation done when calculating the diffusion coefficient for a species with the mixture averaged approximation is that all other species' diffusion velocities are equal, this seems like the place to start an evaluation. This approximation will be less correct the more the velocities differ, which in principle means that the more the masses differ, the less exact the mixture averaged approximation becomes.

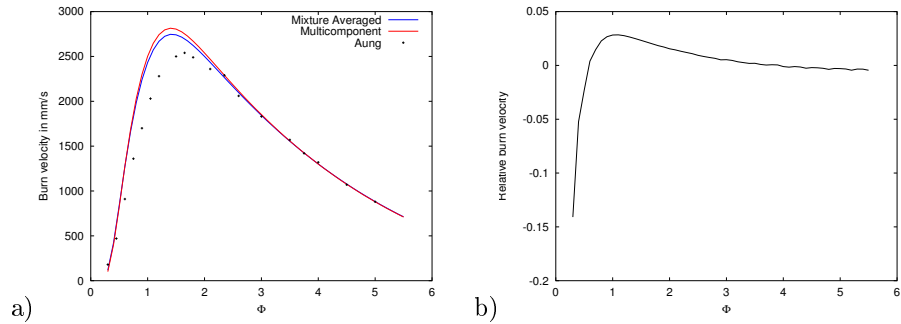


Figure 3.1: a) The calculations compared to Aung's measurements [9]. b) The relative difference in flame speed, $(v_{MC} - v_{MA})/v_{MA}$, as depending on Φ . The pressure and temperature are set to standard values ($T = 298 K$, $P = 101.3 kPa$).

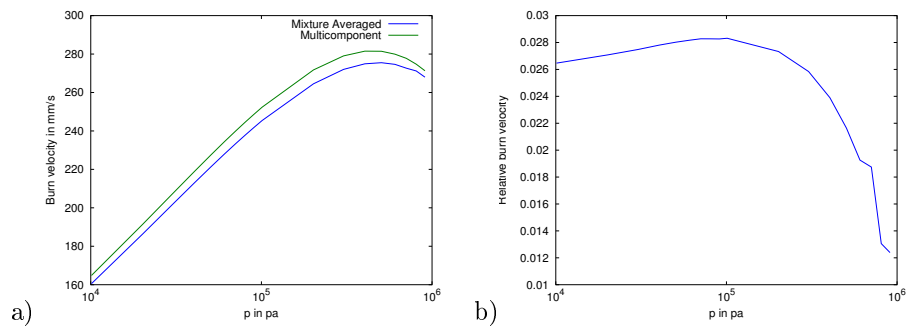


Figure 3.2: a) The flame speed dependence on the initial pressure. The pressure axis is logarithmic. b) The relative difference in flame speeds as a function of the initial pressure.

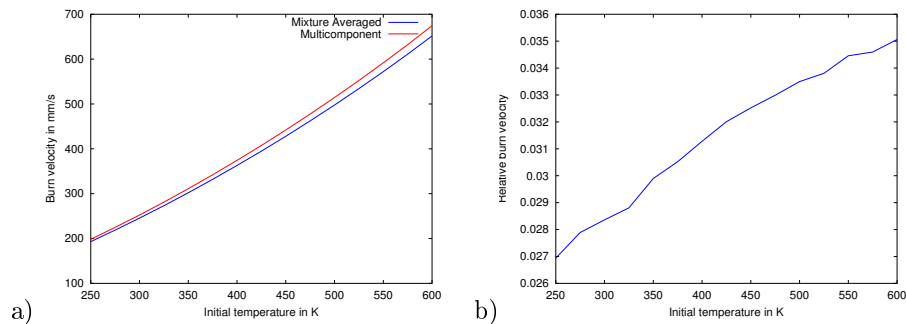


Figure 3.3: a) The flame speed dependence on the initial temperature. b) The relative difference in flame speed as a function of the initial temperature.

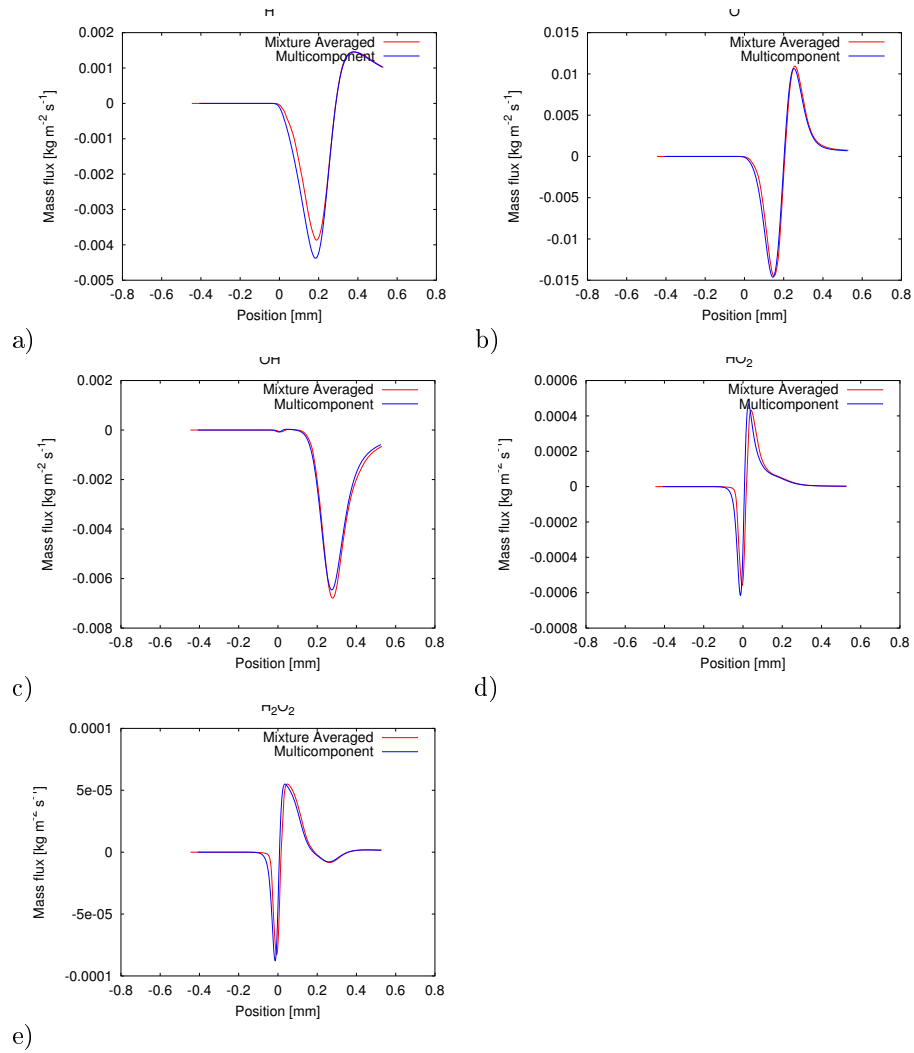


Figure 3.4: The comparison of the diffusion mass flux for the H radical, the O radical, the OH radical, the HO₂ radical and the H₂O₂ radical, respectively.

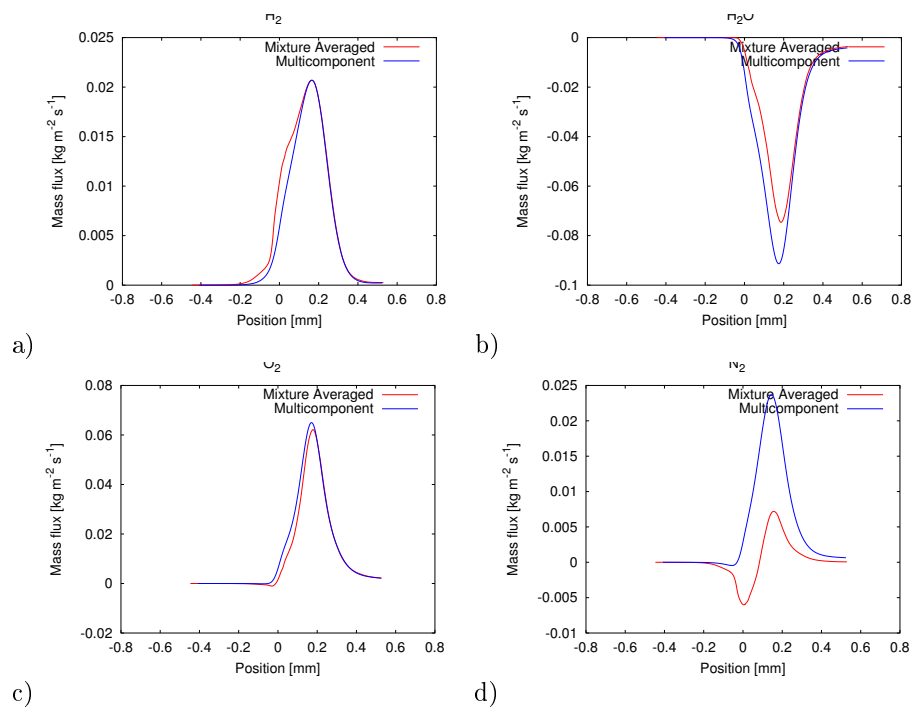


Figure 3.5: The comparison of the diffusion mass flux for the H₂ molecule, the H₂O molecule, the O₂ molecule and the N₂ molecule, respectively.

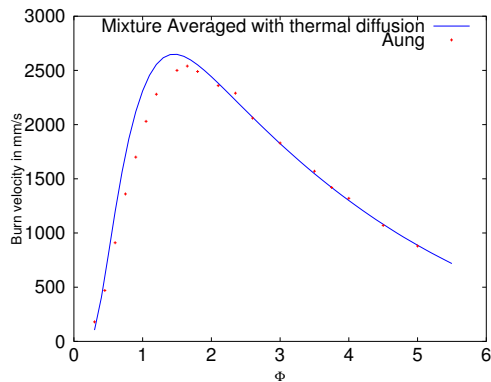


Figure 4.1: Comparison between the mixture averaged model with thermal diffusion, and the experiment from [9]

Since this is an approximation, and it does not take into account that the total mass flux must be zero, it is necessary to apply some correction to make sure that the mass flux is zero, and no mass is lost due to approximations. One way of doing this is via a correction term,

$$j_i = j_i^{MA} - Y_i \sum_j \rho Y_j V_j \quad (4.1)$$

This correction is usually not big enough to return any significant difference, but in slightly more than one percent of the cases in a hydrogen calculation, it is larger than ten percent of the j_i^{MA} .

4.3 Comparison of the Mixture Averaged and the Multicomponent models

As can be seen in the results section above, the two calculations do not give the same results, which is to be expected. If the results were the same, the multicomponent variant would be pointless, since it uses more computational time. The approximation used to derive the mixture averaged approach has been touched on in section 4.2 above, and is not expected to give a major difference, since the mass differences are relatively small. Since the hydrogen combustion is a well-documented area, the mixture averaged calculations should give a result close to the actual values, at least the flame speed. The fact that these simulations are made without thermal diffusion explains quite well why the calculated values deviates from the experimental this much. If thermal diffusion was included, the values would be lower, as can be seen in figure 4.1.

It is good that the multicomponent approach does not deviate to much from the mixture averaged when comparing the flame speed, since that too would imply that the mixture averaged approximation is a bad approximation. And

if it was bad for hydrogen, it would be terrible when heavier species comes into the system, since the larger the difference in mass is, the worse the mixture averaged approximation that all species velocities are the same will be.

The other thing worth noting is the diffusion mass flux for the hydrogen molecules and the nitrogen molecules who's curves were different between the two models. The one with the most apparent difference is the nitrogen, that moves in two different directions according to the mixture averaged approximation, but mainly in one according to the multicomponent model. This behaviour is probably related to the correction term discussed above.

4.4 Comparison to experiment

One major thing to note is how far from the experimental values the calculations end up. That can, at least in part, be explained by the lack of thermal diffusion. Since the thermal diffusion in the multicomponent model is not implemented here, it has been switched off in the mixture averaged model as well, to make comparing them to each other more reasonable. But in doing so, the calculated values are no longer comparable to the experimental, at least not for the region $\Phi \leq 2$. Another fact that further diminishes the relevance of this comparison is the fact that all the chemical values are tuned to work well with the mixture averaged model, and that means that the multicomponent model is at a disadvantage.

The fact that no experimental data to compare the flame speed's dependence on temperature or pressure has been found is not too bad, since it is highly unlikely that they would have ended up close enough to be relevant without thermal diffusion.

4.5 Comparison to other work

The result seen here indicates that the multicomponent model calculates a higher value for flame velocity then the mixture averaged, which is quite the opposite to Bongers and De Goey [10], where the multicomponent gives the best results.

The fact that different chemical files also can give different results can of course also be a contributing factor. Depending on which values the species constants have, the end result will differ. One other thing that can affect the results of these multicomponent calculations compared to the ones made by others are that in this work, the energy levels that relate to rotation have been excluded. This means that all non-reacting collisions are considered elastic, which is not ideal. Exactly how much this affects the end result is hard to say without a deeper examination of this area but it seems unlikely that the effect is large.

5 Conclusion

As has been shown, the multicomponent model comes quite close to the mixture averaged when simulating hydrogen combustion, which seems reasonable. This means that if hydrogen was the only combustion process that was examined, mixture averaged calculations would be the one to use. But since the mixture averaged approximation gets less exact the more the weight ratio between the species increase, the larger molecule velocities involved in the process will be and the less the accuracy of the mixture averaged model will be. And that is why the multicomponent model is considered. In car fuel, one of the standard molecules are octane, weighing more than one hundred times more than the hydrogen radical, that also will be present in the flame region.

This means that the main point of the work presented here will be to enable others to carry on and develop the multicomponent model and implement it in Chamble. What have been shown here is that the mixture averaged is a good approximation for combustion of hydrogen, but it is not identical to the multicomponent. At this time, the work here can only relate to other articles to assess that the multicomponent model is the more precise, but can show some differences in the results.

References

- [1] Digital Analysis of Reaction Systems (DARS), <http://www.loge.se/Products/DARS-products.html> [cited: Jan. 14th 2013]
- [2] Warnatz, J., Maas, U., Dibble, R.W., *Combustion Physical and Chemical Fundamentals, Modeling and Simulation, Experiments, Pollutant Formulation*, 3rd edition, (2001)
- [3] Chapman, S. and Cowling, T.G., *The mathematical theory of non-uniform gases* Third edition, (1995)
- [4] Monchick, L., Mason, E. A., *Transport Properties of Polar Gases*, Journal of Chemical Physics, 35:5, 1676-1697 (1961)
- [5] Law, C. K, *Combustion Physics* (2006)
- [6] Ern, A., Giovangigli, V., *Multicomponent Transport Algorithms* (1994)
- [7] Kee, R. J, Coltrin, M. E. and Glarborg, P., *Chemically reacting flow* (2003)
- [8] Cormen, T. H., Leiserson, C. E., Rivest, R. L. and Stein C., *Introduction to algorithms*, 2nd edition, (2001)
- [9] Aung, K. T., Hassan, M. I. and Faeth, G. M., *Combustion and flame* 109:1-24 (1997)

- [10] Bongers, H. and De Goey, L. P. H., *The effect of simplified transport modeling on the burning velocity of laminar premixed flames* Combustion Science and Technology, 175:10, 1915-1928 (2003)